JPE 3-1-8

P-Q Circle Diagram Based Parameter Measurement for Permanent Magnet Synchronous Motor Including Iron Loss

Naomitsu Urasaki*, Tomonobu Senjyu, and Katsumi Uezato

Dept. of Electrical and Electronics Eng., The University of the Ryukyus, Okinawa, Japan

ABSTRACT

This paper presents parameter measurement for permanent magnet synchronous motors based on the *P-Q* circle diagram Three electrical parameters of permanent magnet synchronous motors, i.e., the equivalent iron loss resistance, armature inductance, and electrical motive force (emf) coefficient are simultaneously measured. The advantages of this method are that it can be implemented under constant excitation and it dispenses with the generating test for the emf coefficient. The proposed method is applied to a 160W permanent magnet synchronous motor, and then the measurement results are analyzed.

Keywords: permanent magnet synchronous motor, parameter measurement, *P-Q* circle diagram, iron loss

1. Introduction

Traditionally, vector controlled ac drives have been performed under the assumption that there is no iron loss in motors. As the employment of vector controlled ac motors, especially induction motor, permanent magnet synchronous motor (PMSM), synchronous reluctance motor has become standard in industrial drives, the improvement of ac motor drives has been important issue. For this reason, several authors have made an attempt to consider the iron loss in vector controlled ac motor drives. The vector controls including the iron loss are investigated for induction motors [1-3] and synchronous reluctance motors [4,5]. The authors have derived a mathematical model of PMSM considering the iron loss under the assumption that the iron loss is produced in equivalent circuit for eddy current. The derived voltage equation newly possesses curious parameter referred to as the equivalent iron loss resistance and the parameter is connected in series with the armature resistance [6]. However, the behavior of the equivalent iron loss resistance has not been revealed experimentally. The objective of this paper is to measure the electrical parameters for this mathematical model and investigate the parameter characteristics with respect to driving frequency in steady-state condition.

As compared with induction motors, parameter measurement for PMSM is a troublesome job because field excitation is constant, i.e., permanent magnet flux is constant. Especially, the iron loss resistance cannot be measure by the no-load test. This paper presents parameter measurement for PMSM based on the *P-Q* circle diagram [7]. The *P-Q* circle diagram can be depicted from the pairs of active power and reactive power when PMSM operates in various load conditions under the constant voltage and

Manuscript received April 1, 2002; revised Nov. 30, 2002.

Corresponding Author: urasaki@tec.u-ryukyu.ac.jp Tel: +81-98-895-8710, Fax: +81-98-895-8708

constant frequency. Electrical parameters of PMSM can easily be calculated from the center and radius of the *P-Q* circle diagram. Three electrical parameters of PMSM, i.e., the armature inductance, emf coefficient and equivalent iron loss resistance are simultaneously measured. The advantages of this method are that it can be implemented under constant field excitation and it dispenses with the generating test for the emf coefficient. The proposed method is applied to a 160W laboratory PMSM, and then the characteristics of driving frequency for these parameters are analyzed.

This paper is organized as follows. The mathematical model of PMSM including the iron loss is reviewed in Section 2. Parameter measurement method by using the *P-Q* circle diagram is presented in Section 3. Parameter measurement results and parameter characteristics are illustrated in Section 4. Some conclusions are given in Section 5.

2. Mathematical Model of PMSM Including Iron Loss

Fig. 1 shows the *d-q* winding model of a PMSM. In this figure, 1*d* and 1*q* represent the armature *d-q* windings, 2*d* the constant field winding corresponding to the permanent magnet mounted on the rotor and 3*d* and 3*q* the equivalent windings for eddy current. In this paper, the iron loss arises from the resistance of the equivalent winding for eddy current[1].

From the *d-q* winding model, the voltage equation for each winding in steady-state condition is expressed as[6]

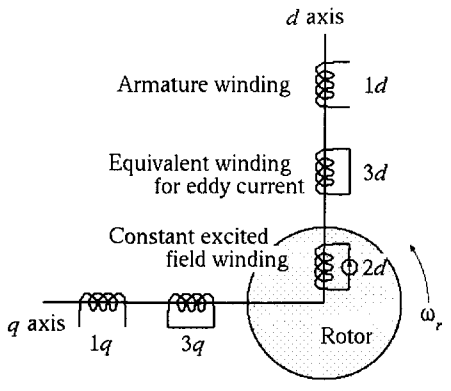

Fig. 1. *d-q* winding model of a cylindrical PMSM.

$$\begin{bmatrix} V_{1d} \\ V_{1q} \\ 0 \\ 0 \end{bmatrix} = \begin{bmatrix} R_1 & -\omega_r L_1' & 0 & -\omega_r M_{13} \\ \omega_r L' & R_1 & \omega_r M_{13} & 0 \\ 0 & -\omega_r M_{13} & R_3 & -\omega_r L_3 \\ \omega_r L_3 & 0 & \omega_r L_3 & R_3 \end{bmatrix} \begin{bmatrix} I_{1d} \\ I_{1q} \\ I_{3d} \\ I_{3q} \end{bmatrix} + \omega_r \begin{bmatrix} 0 \\ M_{12} \\ 0 \\ M_{32}' \end{bmatrix} I_{2d} \quad (1)$$

where, V_1 and I_1 denote the armature voltage and current, respectively. I_2 and I_3 denote the equivalent field current and equivalent eddy current, respectively. ω_r is the electrical angular velocity. R and L denote the each winding resistance and self-inductance, respectively, M is the mutual inductance between windings, and each subscript expresses each winding. Equation (1) is the form that the equivalent eddy currents remain. Since the equivalent eddy currents cannot directly be detected, the equivalent eddy currents should be eliminated by succeeding manipulations.

From (1), the equivalent eddy currents are straightforwardly derived as follows:

$$I_{3d} = \frac{(\omega_r^2 M_{13} L_3 I_{1d} - \omega_r M_{13} R_3 I_{1q} + \omega_r^2 L_3 M_{32}' I_{2d})}{(R_3^2 + \omega_r^2 L_3^2)} \quad (2)$$

$$I_{3q} = \frac{(\omega_r^2 M_{13} L_3 I_{1q} - \omega_r M_{13} R_3 I_{1d} + \omega_r R_3 M_{32}' I_{2d})}{(R_3^2 + \omega_r^2 L_3^2)} \quad (3)$$

Substituting (2) and (3) in (1), the order of the voltage equation can be reduced as,

$$\begin{bmatrix} V_{1d} \\ V_{1q} \end{bmatrix} = \begin{bmatrix} R_1 + R_m & -\omega_r L_1 \\ \omega_r L_1 & R_1 + R_m \end{bmatrix} \begin{bmatrix} I_{1d} \\ I_{1q} \end{bmatrix} + \omega_r \begin{bmatrix} M_{32d} \\ M_{12} + M_{32q} \end{bmatrix} I_{2d} \quad (4)$$

where,

$$R_m = \frac{\omega_r^2 M_{13}^2}{R_3^2 + \omega_r^2 L_3^2} R_3, \quad L_1 = L_1' - \frac{\omega_r^2 M_{13}^2}{R_3^2 + \omega_r^2 L_3^2} L_3$$

$$M_{32d} = \frac{\omega_r M_{13} R_3}{R_3^2 + \omega_r^2 L_3^2} M_{32}', \quad M_{32q} = \frac{\omega_r^2 M_{13} L_3}{R_3^2 + \omega_r^2 L_3^2} M_{32}'$$

The parameter R_m is referred to as the equivalent iron loss resistance and is connected in series with the armature resistance R_1. L_1 denotes the armature inductance. Assuming that the mutual inductances M_{32d} and M_{32q} are sufficiently small as compared with the mutual inductance

M_{12}, these inductances are neglected; as a result, the voltage equation is simplified as,

$$\begin{bmatrix} V_{1d} \\ V_{1q} \end{bmatrix} = \begin{bmatrix} R_1 + R_m & -\omega_r L_1 \\ \omega_r L_1 & R_1 + R_m \end{bmatrix} \begin{bmatrix} I_{1d} \\ I_{1q} \end{bmatrix} + \omega_r \begin{bmatrix} 0 \\ K_e \end{bmatrix} \quad (5)$$

where, K_e (= $M_{12}I_{2d}$) represents the emf coefficient. The validity of this simplification is confirmed by the experimental result illustrated in Section 4.

3. Parameter Measurement by *P-Q* Circle Diagram

The electrical parameters of PMSM are measured based on the *P-Q* circle diagram. In this method, external load is gradually applied to PMSM under terminal voltage with constant amplitude and constant frequency. The input active and reactive powers for each load are measured at that time. Then, the *P-Q* circle diagram is depicted from the pairs of active and reactive powers.

Three electrical parameters including the equivalent iron loss resistance R_m are calculated from the center and radius of the *P-Q* circle diagram. The following illustrates the relationship between the *P-Q* circle diagram and the electrical parameters. Fig. 2 shows the vector diagram for PMSM in steady-state condition. In this figure, ***V*** and ***I*** denote voltage vector and current vector, respectively.

The input active power P and reactive power Q are expressed as,

$$P = VI\cos\varphi \quad (6)$$

$$Q = VI\sin\varphi \quad (7)$$

where, $V = \sqrt{V_{1d}^2 + V_{1q}^2}$, $I = \sqrt{I_{1d}^2 + I_{1q}^2}$ and φ is the power factor angle. From Fig. 2, $I\cos\varphi$ and $I\sin\varphi$ are derived as,

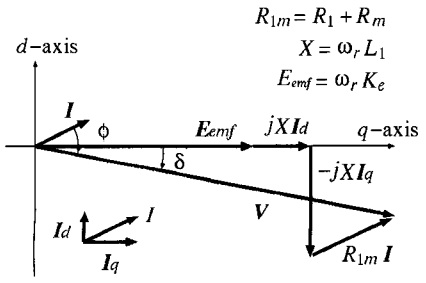

Fig. 2. Vector diagram for PMSM.

$$I\cos\varphi = -I_{1d}\sin\delta + I_{1q}\cos\delta \quad (8)$$

$$I\sin\varphi = I_{1q}\sin\delta + I_{1d}\cos\delta \quad (9)$$

where, δ denotes the load angle. In similar way, $V\sin\delta$ and $V\cos\delta$ are also derived as,

$$V\sin\delta = XI_{1q} - R_{1m}I_{1d} \quad (10)$$

$$V\cos\delta = XI_{1d} - R_{1m}I_{1q} + E_{emf} \quad (11)$$

where, R_{1m}=R_1+R_m, X=$\omega_r L_1$, and E_{emf}=$\omega_r K_e$. Substituting (8) to (11) in (6) and (7), the relationships between the active/reactive power and load angle are derived as,

$$P = P_o + B\sin\delta - A\cos\delta \quad (12)$$

$$Q = Q_o - A\sin\delta - B\cos\delta \quad (13)$$

where, $P_o = \dfrac{R_{1m}}{R_{1m}^2 + X^2}V^2$, $Q_o = \dfrac{X}{R_{1m}^2 + X^2}V^2$,

$$A = \frac{R_{1m}}{R_{1m}^2 + X^2}E_0V,, \quad B = \frac{X}{R_{1m}^2 + X^2}E_0V.$$

Equations (12) and (13) mean that the active and reactive powers vary according to external load conditions even though the input voltage and driving frequency are constant. Furthermore, (12) and (13) give the locus of active and reactive powers with respect to load angle as,

$$(Q - Q_o)^2 + (P - P_o)^2 = R_o^2 \quad (14)$$

where, $R_o = \sqrt{A^2 + B^2}$. This locus expresses the circle with center (Q_o, P_o) and radius R_o illustrated in Fig. 3.

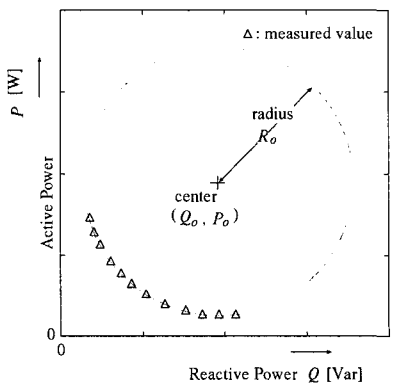

Fig. 3. Principle of *P-Q* circle diagram.

From the parameters P_o, Q_o, A, and B defined in (12) and (13), the relationships between the P-Q circle diagram and electrical parameters are given as follows:

$$R_{1m} = \frac{P_o}{P_o^2 + Q_o^2} V^2 \tag{15}$$

$$L_1 = \frac{Q_o}{P_o^2 + Q_o^2} \frac{V^2}{\omega_r} \tag{16}$$

$$K_e = \sqrt{\frac{R_o^2}{P_o^2 + Q_o^2}} \frac{V}{\omega_r} \tag{17}$$

It is noted that the equivalent iron loss resistance R_m is obtained by subtracting an armature resistance R_1 from the parameter R_{1m}. The armature resistance R_1 is measured by the conventional direct current test in advance. In the proposed method, three electrical parameters of PMSM can be measured simultaneously. In addition, the proposed method dispenses with the generating test for the emf coefficient.

4. Measurement Results

In this section, parameter measurement results based on the P-Q circle diagram are presented and their characteristics with respect to driving frequency are also illustrated. The specifications of the PMSM utilizing in this research are listed in Table 1. Fig. 4 shows the experimental system to execute parameter measurement based on the P-Q circle diagram. In order to measure the electrical parameters on various driving frequencies, a PWM inverter with 7.5 kHz carrier frequency is utilized. A digital power meter detects (DPM) the active power, reactive power, and input voltage. Load conditions for the PMSM is adjusted by changing the external resistance through the generator (PMSG) that connects directly to the PMSM.

Table 1. Motor specifications.

Rated power	160 W
Rated torque	0.5N·m
Rated speed	3000 rpm
Number of pole-pairs	2

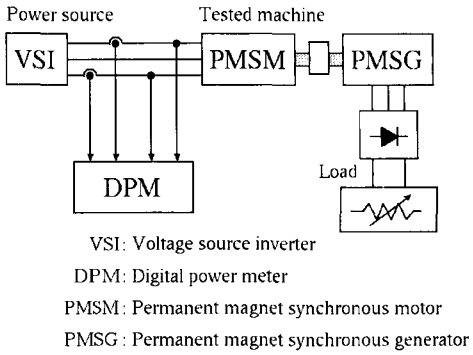

Fig. 4. Experimental system.

Fig. 5 shows a P-Q circle diagram depicted from the pairs of active power and reactive power. In this case, the voltage and driving frequency are 45.5 V and 70 Hz, respectively (V/f = 0.65). Increasing the external load, the measured value moves clockwise on the circle, i.e., the active power increases and reactive power decreases, respectively. Since the experimental system utilizing in this research cannot supply heavy load to PMSM, measured values exist in narrow range on the circle. However, if appropriate load equipment is utilized, they will exist in wide range. From the P-Q circle diagram, the center (Q_o, P_o) and radius R_o are determined as (355.0, 355.0) and 317.5, respectively. The center and radius are decided so as to the emf coefficient by (17) agrees with the emf coefficient by the generating test. Of course, if measured values exit in wide range, the information of the generating test is not required.

Using the values of the center and radius, the equivalent iron loss resistance, armature inductance and emf coefficient are calculated as described in Section 3.

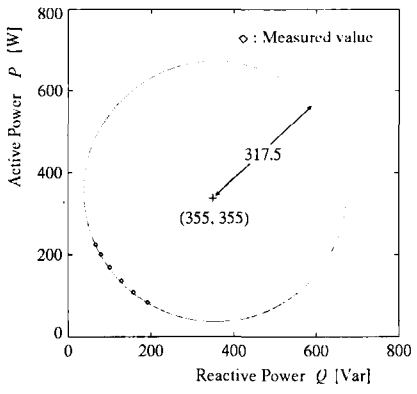

Fig. 5. P-Q circle diagram for 70Hz.

4.1 Equivalent iron loss resistance

The parameter measurement results for the equivalent iron loss resistance R_m, which is introduced newly in voltage equation of PMSM, is discussed in this subsection. The measurement is executed in wide frequency range from 40Hz to 100Hz under various *V/f* ratios. As discussed in Section 3, the equivalent iron loss resistance is calculated by using the center of the *P-Q* circle diagram depicted on each driving frequency.

Fig. 6 shows the equivalent iron loss resistance versus driving frequency. As can be seen from this figure, the equivalent iron loss resistance increases with increasing driving frequency. In order to explain this reason, two assumptions are introduced:

1) Since the eddy current is produced as a result of alternating flux on the armature winding, the leakage inductance of the equivalent winding for eddy current can be considered to be almost zero. Thus, the following relation is satisfied.

$$M_{13} \approx L_1' \approx L_3 \tag{18}$$

2) The resistance R_3 of the equivalent winding for eddy current is much greater than the reactance ωL_3, i.e., the following relation is satisfied.

$$\left(\frac{\omega_r L_3}{R_3}\right)^2 << 1 \tag{19}$$

Using this relation, the equivalent iron loss resistance presented in (4) is arranged as,

$$R_m \approx \frac{\omega_r^2 L_3^2}{R_3} \tag{20}$$

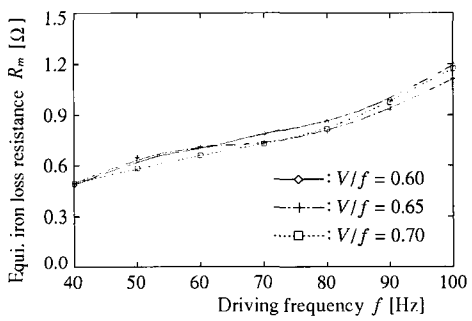

Fig. 6. Equivalent iron loss resistance vs. driving frequency.

As can be seen from (20), the equivalent iron loss resistance increases with increasing electrical angular velocity ω_r (= $2\pi f$), i.e., driving frequency f. It is noted that the driving frequency characteristics of the equivalent iron loss resistance are almost same irrespective of *V/f* ratios.

4.2 Armature inductance

The parameter measurement for the armature inductance L_1 is also executed in wide frequency range from 40Hz to 100Hz under various *V/f* ratios. The armature inductance is calculated by using the center of the *P-Q* circle diagram depicted on each driving frequency.

Fig. 7 shows the characteristics between the armature inductance versus driving frequency. The armature inductance tends to slightly decrease with increasing driving frequency. This reason can be explained as follows: Using the assumption indicated in (18), the armature inductance presented in (4) is arranged as,

$$L_1 \approx \frac{1}{1+\dfrac{\omega_r^2 L_3^2}{R_3^2}} L_3 \tag{21}$$

Furthermore, according to (19), (21) is rearranged as,

$$L_1 \approx L_3 \quad (= \text{Constant}) \tag{22}$$

Thus, the armature inductance can be regarded to be almost constant.

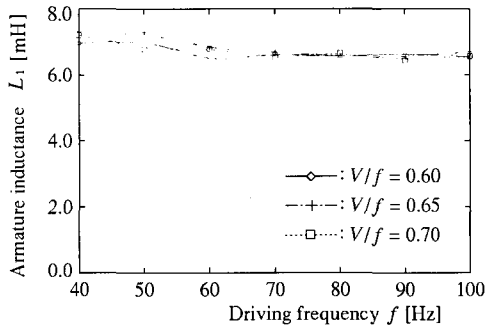

Fig. 7. Armature inductance vs. driving frequency.

4.3 Electromotive-force coefficient

The parameter measurement for the emf coefficient K_e is also executed in wide frequency range under various *V/f* ratios. The emf coefficient is calculated by using the

center and radius of the *P-Q* circle diagram depicted on each driving frequency.

Fig. 8 shows the emf coefficient versus driving frequency. It follows from this figure that the emf coefficient is constant with respect to driving frequency and its characteristics are almost same irrespective of *V/f* ratio. Here, the validity of the simplification in (4) should be confirmed.

From (4), the electromotive force is given as,

$$E_{emf} = \sqrt{M_{32d}^2 + (M_{12} + M_{32q})^2}\,\omega_r I_{2d} \tag{23}$$

In similar with the mutual inductance M_{13}, if the leakage inductance of the equivalent winding for eddy current is almost zero, the following relation is satisfied.

$$M'_{23} \approx M_{12} \tag{24}$$

Thus, M_{32d} and M_{32q} in (4) are rewritten as,

$$M'_{32d} = \left(\frac{\omega_r L}{R_3}\right) M_{12} \tag{25}$$

$$M_{32q} = \left(\frac{\omega_r L}{R_3}\right)^2 M_{12} \tag{26}$$

Using the assumption indicated in (19), (23) is simplified as,

$$E_{emf} \approx \omega_r M_{12} I_{2d} = \omega_r K_e$$

This means that the mutual inductances M_{32d} and M_{32q} are sufficiently small as compared with the mutual inductance M_{12}, i.e., the emf coefficient is constant.

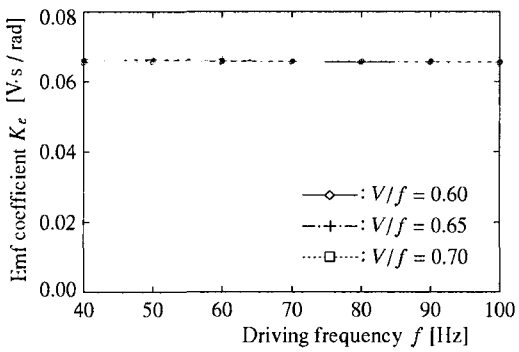

Fig. 8. Emf coefficient vs. drive frequency.

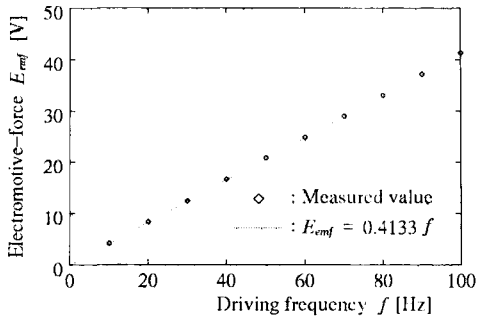

Fig. 9. Electromotive force vs. driving frequency.

Table 2. Electrical parameters.

Proposed method	
Equivalent iron loss resistance R_m	0.69 Ω (f=60Hz)
Armature inductance L_1	6.60 mH
Emf coefficient K_e	0.066 V·s/rad
Traditional method	
Armature resistance R_1	2.13 Ω
Armature inductance L_1	6.50 mH
Emf coefficient K_e	0.066 V·s/rad

Fig. 9 shows the characteristic of electromotive force with respect to the driving frequency obtained by the traditional generating test. This characteristic is linear, \$i.e.\$, the emf coefficient is constant with respect to the driving frequency. This fact validates the simplification in (4).

Parameter measurement results by the proposed method are listed in Table 2. Since the iron loss resistance varies with driving frequency, the measurement result for 60Hz is listed in Table 2. In this result, the iron loss resistance may be over estimated due to increase of the armature resistance with temperature. As can be seen from Fig. 7, the armature inductance is almost constant. The mean value from 70Hz to 100Hz is listed in Table 2. For comparison, the armature inductance by a traditional method is also listed. In the traditional method, the armature inductance is measured by the impedance method. The armature inductance by the proposed method is well agrees with those by the traditional method. As mentioned earlier, the emf coefficient for the proposed method is decided so as to agree with that for generating test (Fig. 9). The advantage of this method is that three parameters can simultaneously be measured. In addition,

the equivalent iron loss resistance is measured under constant field excitation. Furthermore the emf coefficient is measured without the generating test if the measured values exits in wide range on the *P-Q* circle diagram.

5. Conclusions

This paper proposes parameter measurement for PMSM including iron loss. In the proposed method, three electrical parameters of PMSM, i.e., the equivalent iron loss resistance, armature resistance and emf coefficient are simultaneously measured based on *P-Q* circle diagram. This method can be applied to motor with constant field excitation machines such as PMSM. In addition, it dispenses with the generating test for the emf coefficient. The proposed method is applied to a 160W permanent magnet synchronous motor, and then the measurement results are analyzed. The equivalent iron loss resistance increases with increasing driving frequency while the armature inductance and emf coefficient are almost constant. The validity of this proposed method is confirmed by the comparison with the traditional method.

References

[1] T. Mizuno, J. Takayama, T. Ichioka, and M. Terashima, "Decoupling control method of induction motor taking stator core loss into consideration", in Proc. IPEC-Tokyo, pp. 69~74, Tokyo, 1990.

[2] E. Levi, "Impact of iron loss on behavior of vector controlled induction machines", IEEE Trans. Ind. Appl., Vol. 31, No. 6, pp. 1287~1296, Nov./Dec. 1995.

[3] J. Jung and K. Nam, "A vector control scheme for EV induction motors with a series iron loss model", IEEE Trans. Ind. Electron., Vol. 45, No. 4, pp. 617~624, Aug. 1998.

[4] L. Xu, X. Xu, T.A. Lipo, and D.W. Novotny, "Vector control of a synchronous reluctance motor including saturation and iron losses", IEEE Trans. Ind. Appl., Vol. 27, No. 5, pp. 977~984, Sep./Oct. 1991.

[5] A. Vagati, M. Pastorelli, G. Franceschini, and V. Drogoreanu, "Flux-observer-based high-performance control of synchronous reluctance motors by including cross saturation", IEEE Trans. Ind. Appl., Vol. 35, No. 3, pp. 597~605, May/June 1999.

[6] T. Senjyu, T. Shimabukuro, and K. Uezato, "Vector control of synchronous permanent magnet motors including stator iron loss", Int. J. Electronics, Vol. 80, No. 2, pp. 181~190, 1996.

[7] A. Ah. Fock and P.M. Heart, "New Method for Measuring X_d and X_q Based on the *P-Q* Diagram of the Lossy Salient-Pole Machine", Proc. IEE-Elec. Power Appl., Vol. 131, Pt. B, No. 6, pp. 259~262, Nov. 1984.

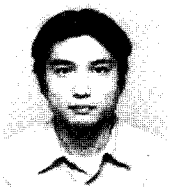

Naomitsu Urasaki was born in Okinawa Prefecture, Japan in 1973. He received the B.S. and M.S. degrees in electrical engineering from University of the Ryukyus, Japan, in 1996 and 1998, respectively. Since 1998, he has been with Department of Electrical and Electronics Engineering, Faculty of Engineering, University of the Ryukyus, where he is currently a Research Associate. His research interests are in the areas of modeling and control of ac motors. Mr. Urasaki is a Member of the Institute of Electrical Engineers of Japan.

Tomonobu Senjyu was born in Saga Prefecture, Japan, in 1963. He received the B.S. and M.S. degrees in electrical engineering from the University of the Ryukyus, Okinawa, Japan, in 1986 and 1988, respectively, and the Ph.D. degree in electrical engineering from Nagoya University, Nagoya, Japan, in 1944. Since 1988, he has been with the Department of Electrical and Electronics Engineering, Faculty of Engineering, University of the Ryukyus, where he is currently a professor. His research interests are in the areas of stability of ac machines, advanced control of electrical machines, and power electronics. Prof. Senjyu is a member of the Institute of Electrical Engineers of Japan.

Katsumi Uezato was born in Okinawa Prefecture, Japan, in 1940. He received the B.S. degrees in electrical engineering from the University of the Ryukyus, Okinawa, Japan, in 1963, the M.S. degree in electrical engineering from Kagoshima University, Kagoshima, Japan, in 1983. Since 1972, he has been with the Department of Electrical and Electronics Engineering, Faculty of Engineering, University of the Ryukyus, where he is currently a Professor. He is engaged in research on stability and control of synchronous machines. Prof. Uezato is a member of the Institute of Electrical Engineers of Japan.